


ORIGINAL ARTICLE

Open Access



Removal of diesel oil from water using biochar derived from waste banana peels as adsorbent

Jeffrick Jun Daniel T. Urgel¹, Justin Marwin A. Briones¹, Emmanuel B. Diaz Jr.¹, Kirstin Margaux N. Dimaculangan¹, Kayla L. Rangel¹ and Edgar Clyde R. Lopez^{2,3*} 

Abstract

Here, banana peel biochar (BPBC) generated from discarded saba banana peels powder (SBPP) was utilized as an adsorbent in this study to remove diesel oil from water. The BPBC was synthesized using a slow pyrolysis method and characterized using SEM, EDX, FTIR, DSC, TGA, BET, contact angle analyzer, and XRD. The results showed that BPBC exhibited high porosity, thermal stability, and hydrophobic character, making it a promising adsorbent for oil-water separation and environmental remediation. The adsorption capacity of BPBC for diesel oil removal was examined in terms of adsorbent dose, pH level, salinity, and contact time. Increasing the BPBC dosage, contact time, and salinity significantly enhanced the sorption capacity, however, pH variations had no significant effect on adsorption. Adsorption parameters were correlated using a reduced cubic model, and an adsorbent dose of 2.50 g, pH of 7.00, salinity of 44,999.95 mg/L, and contact duration of 240 minutes were found to be optimal, producing a sorption capacity of 5.3352 g diesel oil/g adsorbent. The adsorption process was characterized by the first-order kinetic model. The creation of multilayer adsorption on the BPBC surface was confirmed by the BET isotherm. Adsorption characterization revealed changes in the surface morphology, elemental analysis, and functional groups of BPBC after adsorption. SEM revealed occupied surface pores, and EDX analysis verified an increase in carbon content. The presence of adsorbed diesel oil molecules on the BPBC surface was detected by FTIR analysis, which exhibited changes in peak appearance and functional group shifts. Overall, this study presents an adsorbent derived from waste material for diesel oil adsorption, which is useful for remediating oil spills and for wastewater treatment.

Highlights

- Biochar from saba banana peels was used as an adsorbent to remove diesel oil from water.
- The diesel oil solution environmental conditions were optimized to maximize oil adsorption.
- Diesel oil adsorption on biochar follows the first-order kinetic model and the BET isotherm model.

Keywords Oil spill, Adsorption, Biochar, Saba banana peels, Central composite design

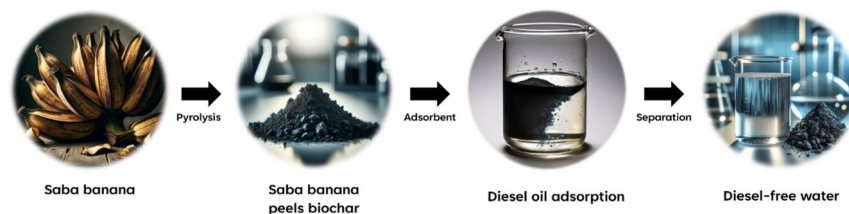
Handling editor: Fengchang Wu.

*Correspondence:

Edgar Clyde R. Lopez
edgarclydelopez09@gmail.com

Full list of author information is available at the end of the article

Graphical Abstract



1 Introduction

Oil spills may be extremely dangerous to marine birds, sea turtles, and mammals, as well as fish and shellfish, depending on the conditions. Oil diminishes the water-repelling ability of bird feathers and the insulating qualities of fur-bearing animals like sea otters, leaving them vulnerable to the harsh climate. Many birds and animals ingest oil and become poisoned when they try to clean themselves or eat greased prey. Additionally, hydrocarbon contamination has a negative impact on both human health and marine life (Cai et al. 2019). The persistent release of hydrophobic pollutants into water bodies, particularly diesel oil resulting from industrial activities, transportation, and accidental spills, has far-reaching consequences on aquatic ecosystems and human health. Diesel oil contains a complex mixture of hydrocarbons, including aromatic and aliphatic compounds, which can disrupt the balance of ecosystems and pose risks to aquatic life. Traditional methods of remediation such as bacterial degradation (Goveas et al. 2022), adsorption using magnetic materials (Qiao et al. 2019) and polymers (Haridharan et al. 2022), use of biosurfactants (Patel et al. 2019), and sorbent devices (Bhardwaj and Bhaskarwar 2018) often involve costly and resource-intensive processes. Thus, there is a growing need for sustainable, cost-effective, and eco-friendly approaches to address diesel oil contamination in water.

One way of achieving a sustainable solution to hydrocarbon pollution in water is by developing new adsorbents from cheap raw materials that can efficiently remove oil from water. Recently, the use of biochar as an adsorbent for oil spill remediation has gained popularity (Pallewatta et al. 2023; Silvani et al. 2017; Zhao et al. 2023). Biochar is a carbon-rich substance created by high-temperature treatment of biomass in an oxygen-free environment, such as hardwood or dung. "Biochar" comes from the terms "bio-" which is "biomass" and "char" to "charcoal." Biochar is characterized by a surface morphology, high specific surface area, and high amounts of functional groupings on the surface, making

it a suitable adsorbent for removing contaminants from aqueous solutions (Kumar and Bhattacharya 2021). Biochar was found to be effective in removing cations and anions from aqueous mixes and organic and inorganic pollutants from water (Ayeni et al. 2020). Biochar was also used for removing oil in wastewater and demonstrated excellent sorption performance (Wei et al. 2024). Compared to activated carbon, biochar has lower production costs and energy consumption. Biochar is a renewable resource and, because of its economic and environmental benefits, is an ideal resource for environmental technologies for treating water pollutants (Dai et al. 2019).

In this study, biochar derived from waste banana peels (BPBC) was used as an adsorbent for diesel oil removal from water. Specifically, saba (*Musa acuminata balbisiana*) banana peels powder (SBPP) underwent slow pyrolysis to produce BPBC. BPBC was characterized using Scanning Microscopy with Energy Dispersive X-ray spectroscopy (SEM-EDX), Fourier transform infrared spectroscopy (FTIR), Differential Scanning Calorimetry (DSC), Thermogravimetric Differential Thermal Analysis (TG-DTA), Brunauer-Emmett-Teller (BET) surface area and pore size distribution analysis, contact angle measurements, and X-ray Diffraction (XRD) analysis. The effects of adsorbent dosage (0.5–2.5 g/L), initial pH (5–9), salinity (500–45,000 mg/L), and contact time (30–240 minutes) on removing diesel oil from the water using BPBC as adsorbent were investigated. Moreover, isotherm and kinetic studies on the adsorption of diesel oil to BPBC were conducted.

Utilizing agricultural waste as a precursor for biochar is innovative as it addresses both waste management and provides a sustainable source for producing an adsorbent material. The application of the biochar derived from banana peels for the removal of diesel oil from water suggests an environmentally friendly approach to remediate water contaminated with diesel oil. This aligns with the growing interest in sustainable solutions for environmental challenges. Moreover, the use of waste banana peels for biochar production aligns with the principles

of circular economy and sustainability. It not only transforms waste into a valuable resource but also offers an eco-friendly alternative for water treatment compared to traditional methods.

2 Methodology

2.1 Production of banana peel biochar (BPBC) from saba banana peels

The gathered banana peels are first prepared by cutting them into little pieces and thoroughly cleaning them in running water before being oven-dried at 100 °C for 24 hours. After the drying process, the raw materials are ground and sieved into 150–300 µm particles to distinguish small particles from bigger particles. The pretreated Saba banana peel or dried banana peel waste with a weight of 989 g is put inside an in-house pyrolysis reactor with a temperature controller and it undergoes 104.2-minute slow pyrolysis at 585.9 °C. These pyrolysis conditions were deemed optimum for the production of the highest yield of biochar from banana peels (Omulo et al. 2019).

2.2 Characterization techniques

Scanning Electron Microscopy and Energy Dispersive Spectroscopy (SEM-EDX, SU3800-Bruker) were used to study the surface morphology and elemental composition of the samples at an accelerating voltage of 3.00 kV. Fourier transform infrared spectroscopy (FTIR, Perkin Elmer Spectrum Two) was also used to detect the functional groups present in the samples. Differential scanning calorimetry (DSC, Perkin Elmer DSC 4000) was used to analyze the thermal characteristics of the samples in a standard aluminum pan from 30 to 430 °C at a heating rate of 10 °C min⁻¹ under 20 mL min⁻¹ N₂ gas. Thermogravimetric Differential Thermal Analysis (TG-DTA, Perkin Elmer STA 6000) from 30 to 900 °C was done at a heating rate of 10 °C min⁻¹ under 20 mL min⁻¹ N₂ gas to determine the weight loss and thermal stability of the samples. The biochar was characterized for its surface hydrophobicity using an in-house contact angle analyzer. The diffraction pattern of BPPBC was obtained using the D8 ADVANCE model of the Bruker X-ray Diffractometer.

2.3 Batch adsorption experiments

Batch adsorption experiments were done at different concentrations of diesel oil in water. A 250-mL beaker is used as a container for batch adsorption. The BPBC is submerged in the beaker containing 200 mL of the oil-water mixture. The set-up is agitated at 200 rpm using a magnetic stirrer. The temperature in all the experiments is fixed at room temperature. Moreover, the agitation rate is maintained at 200 rpm. Contact time was

varied from 30 to 240 minutes according to the experimental design. After adsorption, the BPBC is removed from the mixture by centrifugation, and the concentration of the oil in the solution is measured. The sorption capacity was calculated using Eq. 1. All runs are done three times and the average values are reported.

$$\text{Sorption capacity} = \frac{\text{Mass of BPBC adsorbed} - \text{Mass of BPBC}}{\text{Mass of BPBC}} \quad (1)$$

2.4 Effect of solution environmental conditions on the sorption capacity of BPBC

The adsorption study investigated the effect of four parameters: adsorbent dose, initial pH, salinity, and contact time. Design Expert v.13 (Stat-Ease, USA) is used to create a face-centered central composite design of experiments. The initial adsorbent dose (X_1) is varied from 0.5 to 2.5 g/L, the initial pH (X_2) from 5 to 9, and salinity (X_3) from 500 to 45,000 mg/L, and contact time (X_4) from 30 to 240 minutes. These conditions are based on the typical values observed in various bodies of water (freshwater to marine waters). Six center points were used, yielding a total of 30 runs in the experiment.

Here, synthetic oil-contaminated water is prepared for each run using the initial pH and salinity as indicated in the FCC on CCD. Specifically, appropriate amounts of NaCl are dissolved in 200 mL of distilled water. Then, its pH is adjusted using 1 M HCl or 1 M NaOH. Then, an appropriate amount of diesel oil is added to the solution to produce 100 mg/L of diesel oil in water. This mixture is stirred vigorously at 300 rpm using a magnetic stirrer for 5 minutes. Then, it is sonicated for 10 minutes using a bath sonicator at room temperature. The prepared oil-water mixture is then used for adsorption experiments. Each run is done in three replicates and the average values of the response (sorption capacity) are reported. For each run, the temperature (30 °C), agitation rate (200 rpm), and initial diesel oil concentration (100 mg/L)

Table 1 Levels of the four parameters using face-centered central composite design (FC-CCD)

Independent variables	Unit	Symbol	Levels		
			-1	0	+1
Adsorbent dosage	g/L	X_1	0.5	1.5	2.5
pH	–	X_2	5	7	9
Salinity	mg/L	X_3	500	22,750	45,000
Contact time	minutes	X_4	30	135	240

are held constant. Table 1 shows the different levels that are used in this study.

2.5 Isotherm study

Isothermal adsorption experiments are performed at optimum adsorbent dosage, pH, salinity, and contact time, as determined from the RSM runs. For the isotherm study, the diesel oil concentrations are varied (50 mg/L, 100 mg/L, 150 mg/L, 200 mg/L, 300 mg/L, 400 mg/L, and 500 mg/L).

Synthetic oil-contaminated water is prepared using the optimum initial pH and salinity as determined by FC-CCD. Specifically, appropriate amounts of NaCl are dissolved in 200 mL of distilled water. Then, its pH is adjusted using 1 M HCl or 1 M NaOH. Then, an appropriate amount of diesel oil is added to the solution to produce varying concentrations of diesel oil in water. This mixture is stirred vigorously at 300 rpm using a magnetic stirrer for 5 minutes. Then, it is sonicated for 10 minutes using a bath sonicator at room temperature. The prepared oil-water mixture is then used for adsorption experiments.

For each run, the temperature (30°C) and agitation rate (200 rpm) are held constant. The optimum adsorbent dosage and contact time are used as determined by FC-CCD. Adsorption experiments are then performed under these conditions then the sorption capacity is measured. Each run is done in three replicates and the average values are reported. Several isotherm models are used to determine which equation is the best-fit model based on the obtained experimental data.

2.6 Kinetic study

Adsorption experiments are performed at optimum adsorbent dosage, pH, and salinity, as determined by FC-CCD. However, different contact times are used for the kinetic study (0.25 h, 0.5 h, 1 h, 1.5 h, 2 h, 2.5 h, 3 h, 4 h, and 8 h).

Synthetic oil-contaminated water is prepared using the optimum initial pH and salinity as determined by FC-CCD. Specifically, appropriate amounts of NaCl are dissolved in 200 mL of distilled water. Then, its pH is adjusted using 1 M HCl or 1 M NaOH. Then, an appropriate amount of diesel oil is added to the solution to produce varying concentrations of diesel oil in water. This mixture is stirred vigorously at 300 rpm using a magnetic stirrer for 5 minutes. Then, it is sonicated for 10 minutes using a bath sonicator at room temperature. The prepared oil-water mixture is then used for adsorption experiments.

For each run, the temperature (30°C), agitation rate (200 rpm), and initial diesel oil concentration (100 mg/L) are held constant. Adsorption experiments are performed

under these conditions then the sorption capacity is measured. Each run is done in three replicates and the average values are reported. The sorption capacity of the data points before equilibrium is fitted to the pseudo-first-order and pseudo-second-order kinetic models.

2.7 Statistical treatment

Following the collection of experimental data, the sorption capacity is fitted to a general polynomial model. Then, an analysis of variance (ANOVA) is conducted to identify the terms that have a significant effect on the sorption capacity. Model reduction is done to remove insignificant terms to obtain the final model for the sorption capacity. To identify data outliers, residual analysis is conducted. Influence plots are examined to determine whether any influential data points might distort the model. Contour plots are generated to analyze the effect of the four parameters (adsorbent dosage, pH, salinity, and contact time) on the sorption capacity of BPBC. Finally, optimization is conducted to determine the best conditions to achieve maximum sorption capacity. All of these are conducted using Design Expert v.13 (Stat-Ease, USA).

3 Results and discussion

3.1 Characterization of banana peel biochar (BPBC)

Scanning electron microscopy (SEM) is used to analyze the surface morphologies of saba banana peel powder (SBPP) (Fig. 1) and banana peel biochar (BPBC) (Fig. S1) before the adsorption test. SBPP was examined using a SEM at 500X, 1000X, 5000X, and 10,000X magnification. The SBPP's SEM scans revealed an uneven structure and a porous surface. This could be due to the amorphous nature of the organic raw materials used during pyrolysis. Meanwhile, Fig. 2 shows very porous structures in SEM images of BPBC before adsorption, which can be attributed to the pyrolysis procedure (Silva et al. 2022). Pyrolysis carbonizes the carbonaceous raw materials used, which creates a large number of pores suitable for adsorption. Indeed, following the pyrolysis of the banana peels, the biochar contains a large number of adsorbent surfaces capable of adsorbing molecules (Sial et al. 2019). This is expected given that the BPBC is pyrolyzed at 585.9°C for 104.2 minutes.

The findings of evaluating the elemental composition of the SBPP and BPBC using energy dispersive X-ray spectroscopy (EDX) point analysis are shown in Table S1. According to Sial et al. (2019), biochar generated from banana peel waste has a high potassium (K) content, similar to what has been observed in this study. Other elements, such as aluminum, magnesium, and chlorine, remained constant before and after biochar formation. The wt.% composition of BPBC shows that the biochar is

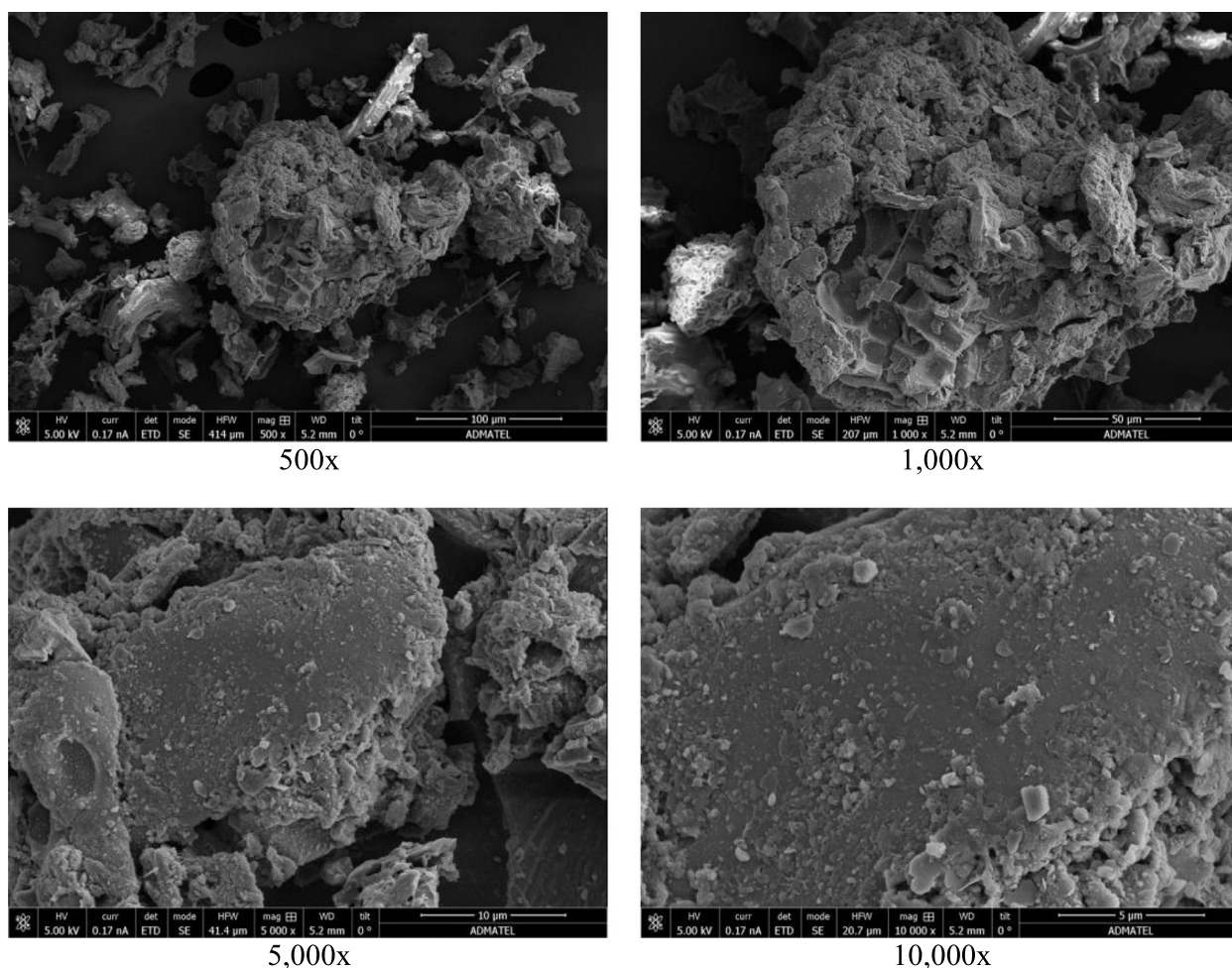


Fig. 1 Scanning electron microscopy (SEM) images of banana peel biochar (BPBC) at different magnifications

mostly composed of carbon, which is expected because the source material, banana peel, is high in carbon. The carbon content of the SBPP decreased when it transformed to BPBC during pyrolysis. This can be attributed to the release of gases such as carbon dioxide, methane, and others. The release of these gases can contribute to the reduction in carbon content as they are in gaseous form and are no longer part of the solid biochar.

SBPP and BPBC were subjected to Fourier transform infrared spectroscopy (FTIR) to determine the surface's functional groups and the results are shown in Fig. 2a. The SBPP peak at 1610 cm^{-1} and in the BPBC at 1576 cm^{-1} can be attributed to C=C stretching due to α , β -unsaturated ketone compounds consisting of a carbon-carbon double bond, which is chemically reactive and capable of undergoing a variety of reactions, including addition reactions, conjugate additions, and polymerization. Meanwhile, the peaks at 1243 cm^{-1} in SBPP and the peak at 1059 cm^{-1} in BPBC can be attributed to the C-O stretching of an aromatic ester.

SBPP contains peaks at 2919 cm^{-1} and 2853 cm^{-1} , while BPBC has a peak at 2921 cm^{-1} . These peaks are caused by the stretching vibrations of the hydroxyl groups, which may be due to the presence of carboxylic groups in both samples.

Differential Scanning Calorimetry (DSC) was used to determine the thermal properties of the SBPP and BPBC (Fig. 2b and Table S2). Endothermic peaks are seen at $Tp_1 = 86.09^\circ\text{C}$, $Tp_2 = 130.17^\circ\text{C}$, $Tp_3 = 157.29^\circ\text{C}$ and $Tp_4 = 388.28^\circ\text{C}$ for BPBC. The endothermic peaks are seen at $Tp_1 = 82.09^\circ\text{C}$ and its exothermic peaks at $Tp_2 = 297.51^\circ\text{C}$, and $Tp_3 = 413.10^\circ\text{C}$ in SBPP. The shift in transition temperatures between SBPP and BPBC can be attributed to an enhanced crystallinity of the BPBC after the pyrolysis of SBPP. Greater crystallinity is desired since it indicates that the material is better structurally organized and thus more stable (El-Nemr et al. 2021). BPBC also has larger endothermic peaks, indicating that it is more thermodynamically stable than SBPP.

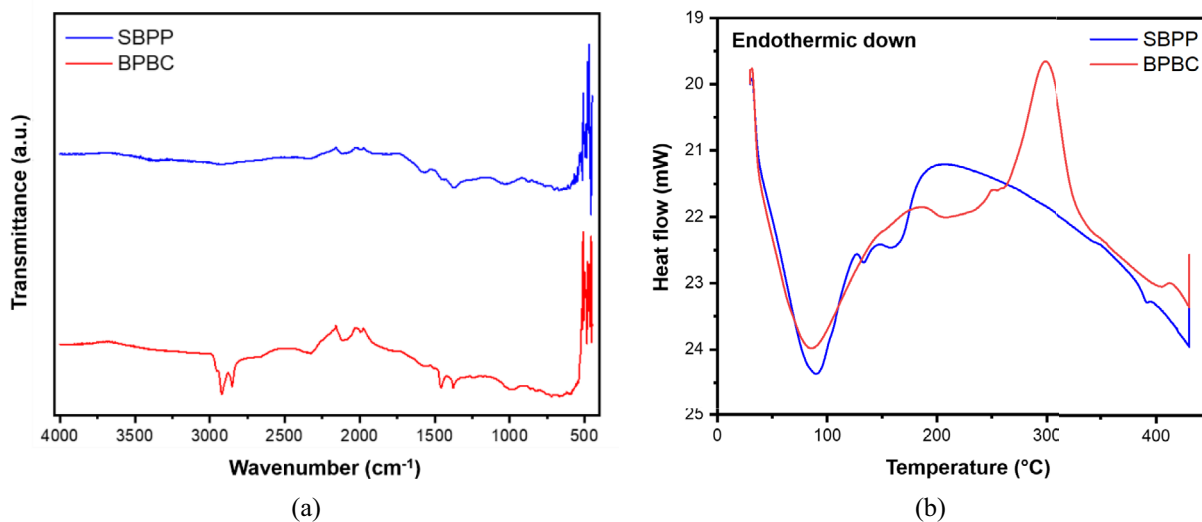


Fig. 2 **a** Fourier transform infrared (FTIR) spectra of saba banana peel powder (SBPP) and banana peel biochar (BPBC) before adsorption; **b** Differential scanning calorimetry (DSC) profiles of SBPP and BPBC before adsorption banana peel at 886 cm^{-1} and BPBC before at 879 cm^{-1} indicated the starch's organized or crystalline structure. The ortho-substituted aromatic rings' C-H out-of-plane bending vibrations were allocated to the band (Sinanoglou et al. 2023). The 1733 cm^{-1} and 1712 cm^{-1} stated the C-H bending; this indicates that bending vibrations arise from the bending motion of the hydrogen atoms attached to the carbon atoms in the aromatic ring. The C-H bending in dried banana peel peak at 1450 cm^{-1} is from a methyl group; this shows that dried banana peel is still an organic material, and some moisture has been evaporated, which is a genuine base from the previous statement; this cannot be seen in BPBC. That dried banana peel is still an organic material, and some moisture has evaporated but can be seen using FTIR

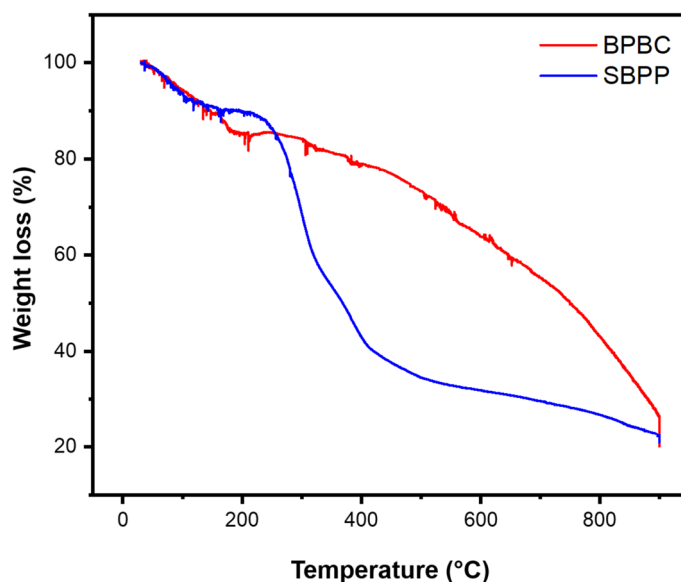


Fig. 3 Thermogravimetric profile of saba banana peel powder (SBPP) and banana peel biochar (BPBC) before adsorption

Thermogravimetric analysis (TGA) was performed on the SBPP and the BPBC (Fig. 3 and Table S3). The SBPP total weight loss of 9.897% observed from $30.00\text{ }^{\circ}\text{C}$ to $65.24\text{ }^{\circ}\text{C}$ could be attributed to the vaporization of low-molecular-weight compounds. The weight loss of

36.603% from $65.24\text{ }^{\circ}\text{C}$ to $142.28\text{ }^{\circ}\text{C}$ could be due to the thermal degradation of the cellulose and hemicellulose content of BPBC. The third stage, with a weight loss of 31.179% from $142.48\text{ }^{\circ}\text{C}$ to $290.32\text{ }^{\circ}\text{C}$, shows that the cellulose and hemicellulose continue to decompose via

pyrolysis reactions. The last stage has a big slope; indicating the thermochemical conversion of SBPP to BPBC. At this temperature range, cellulose and hemicellulose break down mostly. The products created undergo several simultaneous reactions, which result in the generation of gaseous and liquid products. This phase of pyrolysis is frequently referred to as the active phase.

The SBPP and BPBC show the acceleration of lignin breakdown in the last section. The products created undergo several simultaneous reactions, which result in the generation of gaseous and liquid products. The section with inflection found at lower heating rates is absent at the greatest heating rate, where there is a continual, gradual change in the percentage of weight loss and conversion in the temperature. This behavior may be linked to an increase in the production of active species as a result of cellulose's thermal degradation, those species' interactions with one another and with lignin, and the lignin's progressive breakdown that results in the development of char (Kumar et al. 2019).

The first slope of decomposition of BPBC ends at 222.33 °C, which is longer compared to dried banana peel at 170.83 °C. The DTG profile showed that the maximum weight loss peak shifted from 533.23 °C from the BPBC to 290.32 °C from the dried banana peel. The BPBC residue percentage is 57.951%, while the dried banana peel contains 22.321%. This shows that BPBC is more stable than a dried banana peel. Another indication of this is the fact that dried banana peel yielded less residue after TGA in BPBC. Biochar's characteristics are influenced by the feedstocks it is made from, and biomasses with a disproportionately high quantity of lignin and cellulose tend to provide biochar with a high aromatic carbon content.

The results of BPBC showed that it was more stable than SBPP. This agrees with the results in FTIR and DSC, which showed higher crystallinity that could result in more thermal stability than a dried banana peel. BPBC can be exposed to a wider range of operating temperatures, and it undergoes pyrolysis, which enhances the banana peel's stability. The thermal stability creates more carbon that is useful in adsorption.

BET studies (Fig. 4) show the physical assessment of BC pyrolysis, which is often related to their sorption properties. When considering BPBC as an adsorbent, the surface area and pore volume are critical parameters. Biochar derived from *Musa acuminata balbisiana* had a surface area of 3.65 m²/g and a pore volume of 0.032 cc/g. At the same pyrolysis temperature, other studies show that it has a comparable surface area with other biochars (Selvarajoo et al. 2020). When the micropore volume of the BC was compared, the BPBC had a substantially higher micropore volume (3.3154 × 10⁻² cc/g): BCs made

from durian has 8.587 × 10⁻³ cc/g and biomass of palms has 0.0209 cc/g (Elnour et al. 2019).

The pore size distribution of the BPBC is shown in Fig. 5c. Based on the pore size distribution, it can be inferred that the BPBC has a hierarchical pore structure with micropores, mesopores, and macropores. The average pore diameter of BPBC is 36.298 nm, which is somehow larger compared to other BCs derived from biomass. BCs from commercially available product Douglas fir have a pore volume of 0.26 cm³/g and an average pore diameter of 13.95 nm; modified from lauric acid (LBC) has a pore volume of 0.26 cm³/g and an average pore diameter of 14.47 nm; modified from iron oxide (MBC) has pore volume of 0.135 cm³/g and average pore diameter of 13.56 nm; LBC modified with iron-oxide (LMBC) has pore volume 0.014 cm³/g and average pore diameter of 14.52 nm; and MBC modified with lauric acid has a pore volume of 0.016 cm³/g and average pore diameter of 4.30 nm.

The XRD profile of the biochar samples is shown in Fig. 5. Numerous mineral phases were present, as evidenced by the study of the XRD patterns. Graphite, with a characteristic peak of 24.22°, 28.33°, and 30.06°, was the most recognizable crystallographic structure. The peak in 31.21°, 31.39°, 31.76°, 34.09°, 39.24°, and 40.48° represents turbostratic graphite. The graphite indicates that the biochar material contains crystalline graphite. The existence of structured carbon structures or partly graphitized carbon inside the biochar is proven by the detection of graphite, which is distinguished by its highly ordered and layered crystal structure. Because biochar goes through high-temperature pyrolysis, the graphitization of carbon is visible. The existence of turbostratic graphite in X-ray diffraction (XRD) peaks reveals a disordered arrangement of graphene layers in the carbon structure. The disorder in the graphite layers, which causes differences in the interlayer spacing and orientations of the graphene sheets, is the cause of the shortness of the peaks. The degree of peak shortening and the relative strength of the dispersed peaks can be used to determine the degree of disorder.

The contact angle test was used to evaluate the ability of BPBC to absorb oil in water by measuring its surface hydrophobicity using a contact angle analyzer (Fig. 6). The BPBC was positioned on the stage of the contact angle analyzer, and a droplet of water was slowly dropped with a pipette. The contact angle average is 98.45°, indicating that it displays hydrophobic characteristics. The hydrophobicity of the BPBC possesses a low affinity for water due to their nonpolar structures. This property allows them to detach from water and interact with hydrophobic oil molecules. The high affinity of hydrophobic materials with oil facilitates stable surface

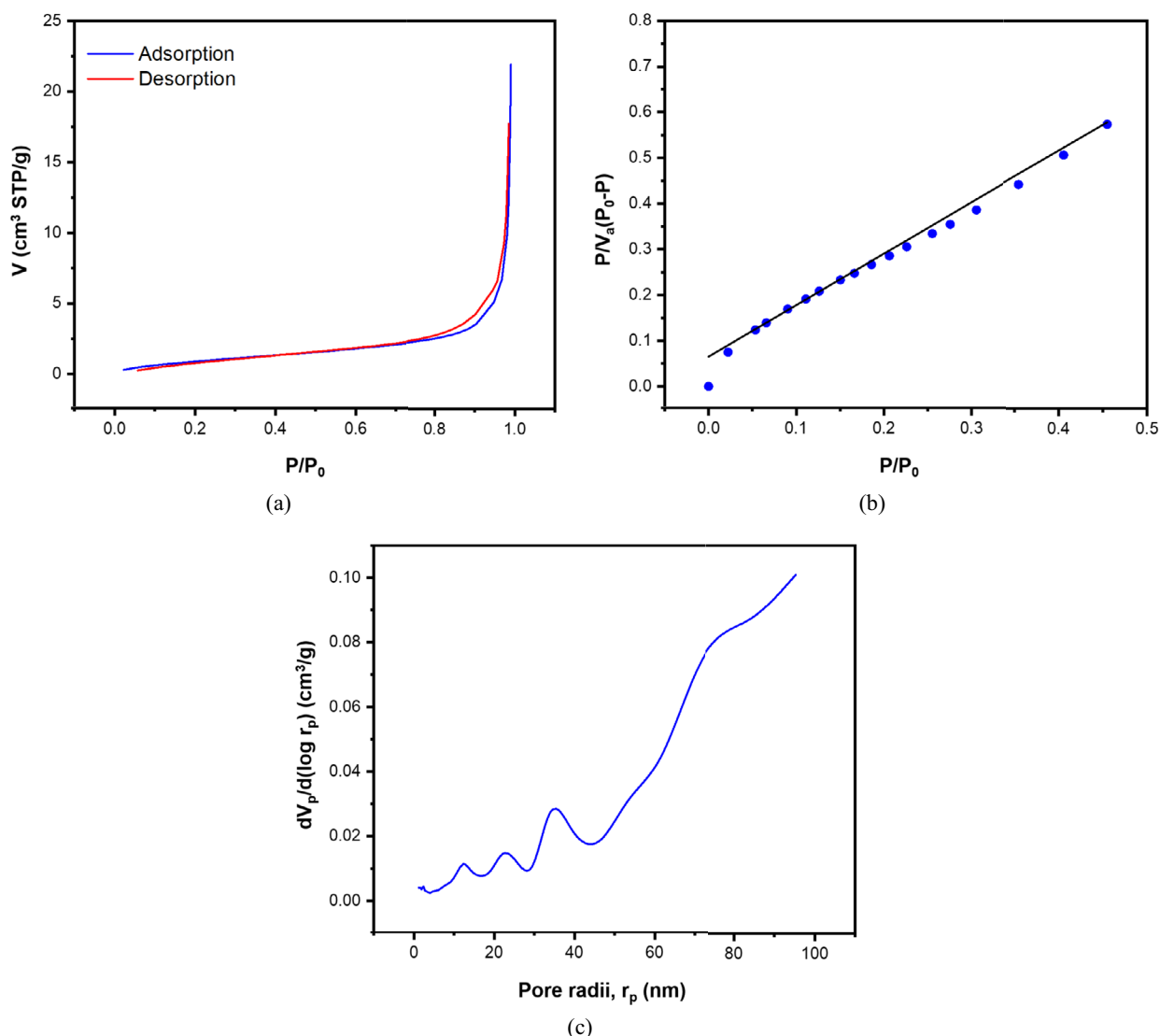


Fig. 4 **a** Nitrogen adsorption-desorption profile, **b** Brunauer-Emmett-Teller (BET) fit of N₂ sorption isotherm, and **c** Pore size distribution of banana peel biochar (BPBC)

interactions and adsorption of oil molecules (Sun et al. 2011). Additionally, hydrophobic adsorbents have large surface areas and porosity, as seen from our BET and SEM characterization, which further enhance their ability to interact and adsorb oil molecules.

3.2 Effect of solution environmental conditions

We studied the effect of solution environmental conditions on the sorption capacity of BPBC. Based on the findings, the highest sorption capacity is observed at a loading of 2.5 g of adsorbent, whereas the lowest capacity is observed at a loading of 0.5 g. The significance of the adsorbent dosage is supported by the ANOVA, with

a p -value of 2.3149×10^{-6} . Fig. 7a illustrates an upward trend in sorption capacity as the adsorbent loading increases. The effectiveness of the process relies on the amount of biochar available for adsorption, which is determined by the adsorbent dose. Initially, a low dose of adsorbent may result in reduced removal efficiency due to limited surface area for adsorption. However, increasing the dosage improves the removal efficiency. Additional biochar provides more surface area and accessible adsorption sites for diesel oil molecules, leading to a higher removal capacity from water.

The sorption capacity of BPBC exhibits distinct variations with changes in pH. The highest sorption capacity is

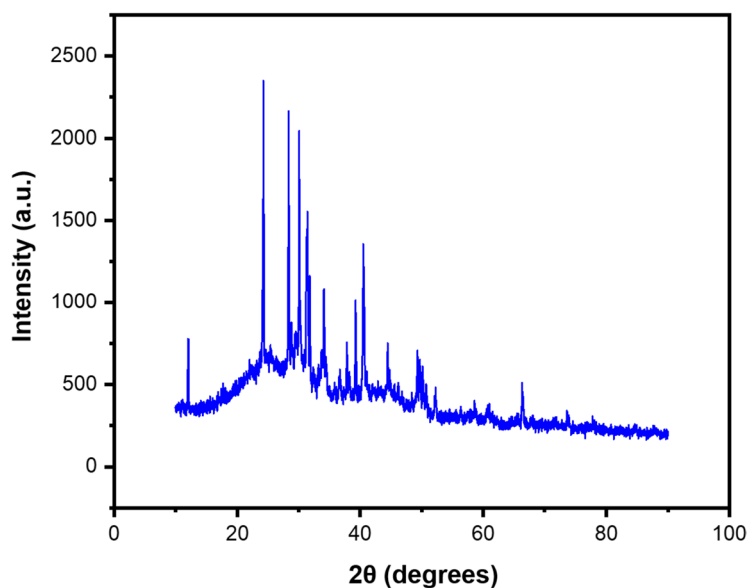


Fig. 5 X-ray diffraction (XRD) profile of banana peel biochar (BPBC)

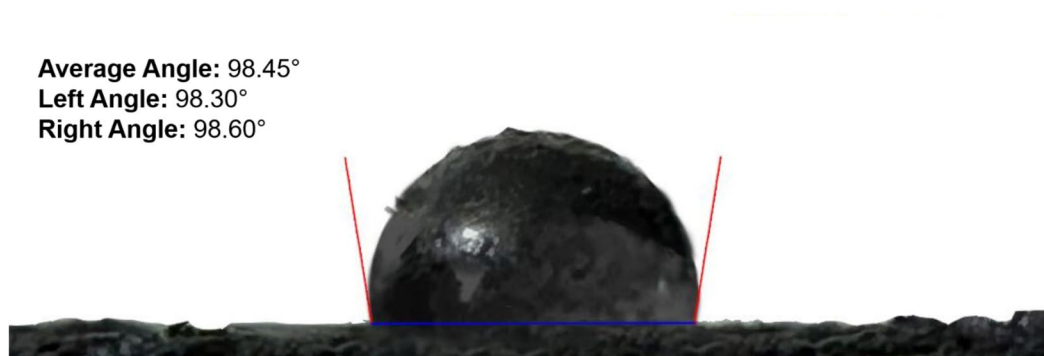


Fig. 6 Contact angle test of banana peel biochar (BPBC)

observed at pH7, indicating optimal conditions for maximum adsorption efficiency, whereas the lowest sorption capacity is observed at pH5. To ascertain the statistical significance of pH on the adsorption process of BPBC, an analysis of variance (ANOVA) was performed. The results revealed that the variation in pH does not have a significant effect on the adsorption of BPBC from oil and water ($p=0.6830$). However, while the statistical analysis did not reveal a significant effect, the observed changes in sorption capacity at different pH levels are nonetheless relevant as they provide vital insights into the behavior of BPBC. This concave downward trend is visually depicted in Fig. 7b, suggesting that further increases in pH beyond 7 do not lead to any additional enhancement in sorption capacity. Since pH lies in its ability to modify the charges of both the adsorbent material and the pollutants present in the system. By altering these charges, pH can

influence the adsorption behavior of BPBC (Grisales-Cifuentes et al. 2021). Initially, at lower pH values, there is an effective interaction between BPBC and diesel oil due to favorable charge interactions. As the pH increases beyond a certain point, the charge interactions may reach a saturation point, resulting in a diminished rate of increase in sorption capacity. This saturation effect could explain why the sorption capacity at pH9 returns to the level observed at pH5.

The salinity levels utilized in all trials were 500, 22,750, and 45,000 mg/L⁻¹. The results show that the lowest sorption capacity is at 500 mg/L and the highest capacity is at 45,000 mg/L of salinity. ANOVA, with a p -value of 3.2424×10^{-6} , supports the importance of the salinity in the adsorption process. As the salinity rises, the sorption capacity shows an ascending trend, as shown in Fig. 7c. The biochar's capacity to absorb can be increased

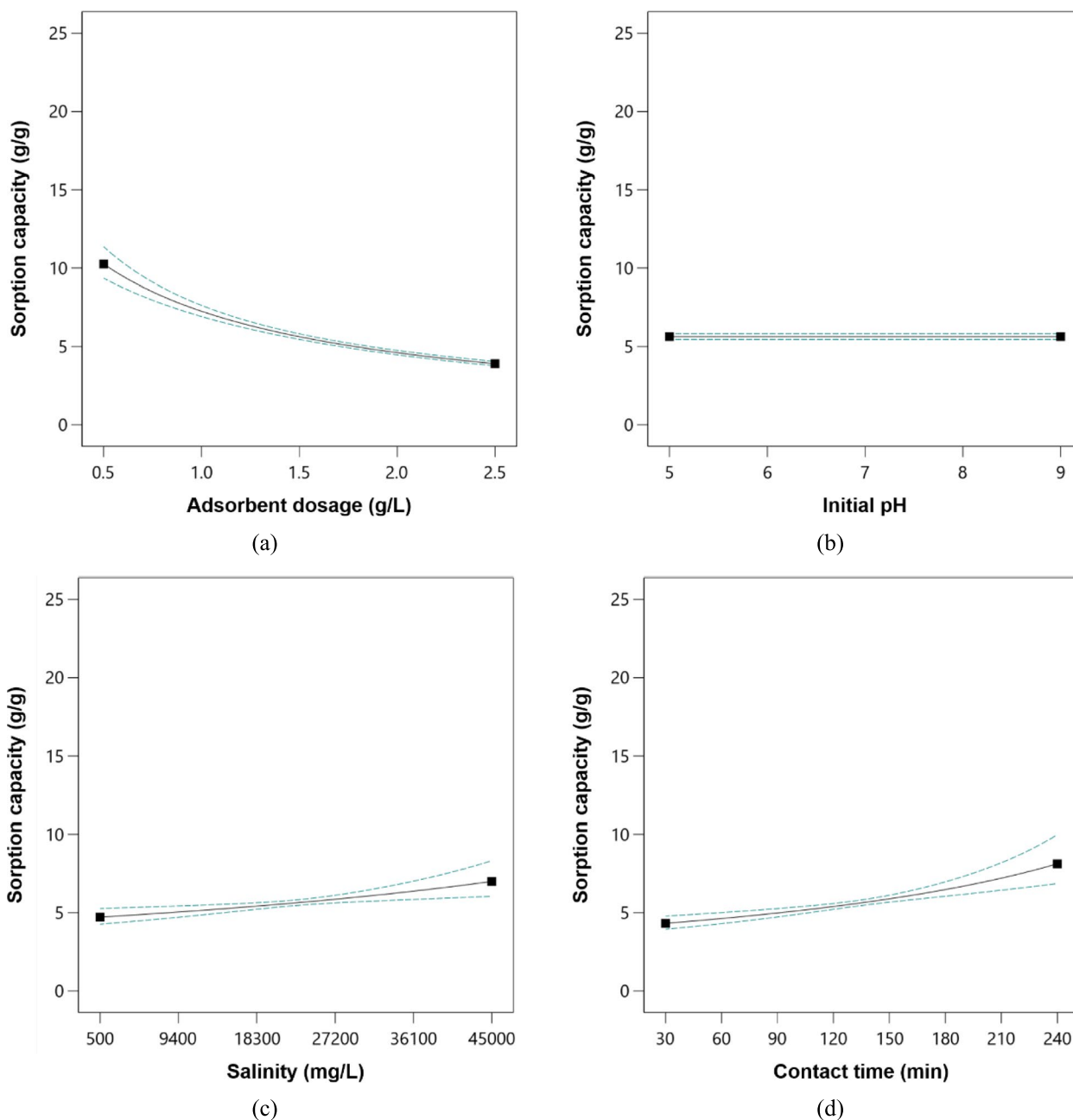


Fig. 7 Effect of adsorption parameters on the sorption capacity of banana peel biochar (BPBC): **(a)** adsorbent dosage, **(b)** initial pH, **(c)** salinity, and **(d)** contact time

by higher salinity for a variety of reasons. Salinity may alter the biochar’s surface charge and functional groups, influencing its affinity for diesel oil molecules. Changes in surface chemistry can impact the adsorption capacity. Biochar has a large surface area and includes functional groups that can interact with the ions in the saline solution via electrostatic interactions. The double-layer thickness around the biochar particles can be influenced

by the water’s ionic strength, which in turn can impact the attractive or repulsive interactions between the oil molecules and the adsorbent. This in turn may have an impact on the biochar’s ability for sorption. Moreover, waste banana peels are used to make biochar, which has a variety of surface functional groups like hydroxyl (–OH) and carboxyl (–COOH) groups. In oil sorption, these functional groups are crucial. The ionic strength of

oil adsorption using biochar can be affected by salinity. Nonpolar functional groups are also present, which contributes to hydrophobic interactions. By changing the pH and ionic strength of the solution, salinity can affect the accessibility and availability of certain functional groups. The surface chemistry of the biochar can change as a result of salinity changes in the solution, which will then have an impact on how well the biochar can absorb oil.

The significance of contact time was established using ANOVA ($p=8.1786 \times 10^{-7}$); the fact that it is less than 0.05 indicates that the adsorption of BPBC from oil and water has a substantial impact. The 30-minute contact time yields the lowest, and 240 minutes lead to the maximum grams of sorption, respectively. As a result, 240 minutes lead to the higher sorption capacity at 5.4530 g. Fig. 7d shows how sorption capacity tends to rise as contact time rises. It indicates that longer contact times are often employed to examine the equilibrium adsorption capacity of biochar. Equilibrium is reached when the rate of adsorption becomes equal to the rate of desorption, resulting in a stable concentration of adsorbate (in this case, oil) on the biochar surface. The diffusion and mass transfer of diesel oil molecules from the bulk solution to the surface of the biochar are affected by the contact time. Adsorption is more likely when contact periods are longer because the diesel oil has more time to permeate through the water and come into touch with the biochar particles. As time passes, the adsorption increases. Oil molecules may transfer slowly from the liquid phase onto the adsorbent surface. Low oil solubility, diffusional restrictions, or insufficient mixing/agitation can all contribute to this (Mokhatab et al. 2019). A progressive rise in the sorption capacity results from lengthening the contact period, giving more time for mass transfer. At a particular time, the inactive sites or surfaces of BPBC get activated and acquire a solution to get saturated. The space in between, or the porosity of the BPBC, is being occupied as time passes. The active sites where the adsorption takes place take time to cover, and with the attaching force acting on the biochar, adsorption coverage increases further as time proceeds. As the contact period lengthens, a saturation of the adsorption sites may occur, signaling the adsorption process's maximal efficiency.

3.3 Statistical treatment

$$\begin{aligned} \text{Sorption capacity} = & 2.01338 - 1.29494[X_1] - 0.000025[X_3] + 0.004601[X_4] + 0.000075[X_1X_3] \\ & - 1.44820 \times 10^{-8}[X_3X_4] + 0.744650[X_1]^2 - 0.002074[X_2]^2 + 8.06857 \times 10^{-6}[X_4]^2 \\ & - 3.44540 \times 10^{-8}[X_1X_3X_4] - 0.000021[X_1^2X_3] + 0.000047[X_1^2X_4] + 0.000191[X_1X_2^2] \quad (2) \end{aligned}$$

where Sorption capacity is in g/g, X_1 =adsorbent dosage (g/L), X_2 =pH, X_3 =salinity (mg/L), and X_4 =contact time (minutes).

The relevance of each parameter in the adsorption of oil in biochar was determined using ANOVA. In this statistical test, p -values greater than 0.05 suggest that there is a statistically insignificant difference in that group, while p -values less than 0.05 indicate that the findings are significant. The ANOVA results revealed that the main effects of adsorbent dose (X_1), salinity (X_3), contact duration (X_4), linear interaction effects (X_1X_3 , and X_3X_4), quadratic effects (X_1^2 , X_2^2 , and X_4^2), and cubic effects ($X_1X_3X_4$, $X_1^2X_3$, and $X_1X_4^2$) are the significant variables in the model. All other model terms have p -values more than 0.05; they have insignificant effect on oil adsorption in biochar. All insignificant model terms are removed from the cubic model and the results are shown in Table S4. The reduced cubic model used to fit the experimental data in terms of actual components is shown in Eq. 2.

The coefficient measurements and values in the coded equation show how each parameter influences the final result. The coded equation may be used to identify the relative significance of the elements by comparing the factor coefficients. X_3X_4 , X_2^2 , $X_1X_3X_4$, $X_1^2X_3$, and $X_1^2X_4$ have negative values, suggesting antagonistic effects on the response, whereas the others have positive values. The reduced cubic model presented in Table S4 demonstrates a highly significant type F-value of 61.05 and a low model p -value of 1.1094×10^{-33} . These findings suggest that the selected reduced cubic model effectively predicts the oil adsorption proportion in biochar within the specified range. It is worth noting that an F-value of this magnitude would only occur due to chance 0.01% of the time, indicating a strong relationship. Moreover, the lack-of-fit analysis reveals an F-value of 0.6265 and a corresponding p -value of 0.8979, indicating that the lack of fit is not statistically significant. This non-significant lack of fit is desirable because it means that the reduced cubic model can be reliably used to forecast biochar sorption capacity.

A greater coefficient, in general, suggests a better fit for the model. Here in this research, the significant coefficient of determination ($R^2=0.9071$) of the model is high, suggesting that it can adequately explain the differences in the experimental data. The coefficient of determination is a value between 0 and 1 that indicates how effectively a statistical model predicts a result, but it is near 1.00

when the final model can appropriately match the experimental data. The adjusted R^2 (0.8923) and predicted R^2 (0.8644) are both close to 1.00, indicating that the model is not overfitted. The calculated model adequacy value (24.8000), which measures the signal-to-noise ratio, is more than 4, indicating that the cubic model can anticipate the response and the pure error of prediction within the design space adequately. Such outcomes demonstrate the model's ability to fit the experimental data.

3.4 Optimization of adsorption parameters

Since the model has a high coefficient of determination, the model fits well with the experimental data. This means that it can reliably predict the sorption capacity of the BPBC at varying levels of solution environmental conditions within the selected design space. As such, the model is robust enough and can therefore be used for optimization studies. Here, we maximized the BPBC sorption capacity, minimized the model error, and maintained the solution environmental conditions within the limits of the design space. Numerical optimization was performed using Design Expert v. 13.0. It was determined that 2.50 g BPBC loading, pH 7.00, 44,999.95 mg L⁻¹ salinity, and 240 minutes of contact time were the optimum parameters for diesel oil adsorption. Under these conditions, biochar has a sorption capacity of 5.600 g/g. The biochar made from banana peels is an excellent material for adsorbing oil with water because it has a highly anticipated ability to adsorb oil under optimal conditions. On the other hand, blank and control experiments showed negligible oil adsorption/separation.

3.5 Kinetic study

We performed a kinetic study on BPBC diesel oil adsorption using the first-order and second-order kinetic models for each diesel concentration (Fig. S2). According to the R^2 value (Table 2), the first-order model offers a better fit to the data points than the second-order model. It

implies that the relationship between the adsorbate concentration and the adsorption rate is better described by first-order kinetics than by second-order kinetics. The experiment shows that adsorbate (diesel oil) binds to the adsorbent surface more quickly at first, speeding up the adsorption process, and the adsorbate gradually attaches to the open adsorption sites on the adsorbent surface; such process goes on for a more extended period. The model assumes that adsorption occurs on a single layer of adsorbate molecules on the surface of the adsorbent. This also assumes that the adsorbent surface is homogeneous and that multilayer adsorption or interactions between adsorbate molecules are negligible. Moreover, the model assumes that the concentration of the adsorbate in the bulk solution remains approximately constant during the adsorption process. This assumption implies that the adsorption sites on the adsorbent surface are close to the bulk solution, allowing for rapid equilibration. Furthermore, the model assumes that all adsorption sites on the surface of the adsorbent are identical in terms of their affinity for the adsorbate. Also, the desorption of the adsorbate from the adsorbent surface is negligibly compared to the rate of adsorption. This assumption implies that once the adsorbate molecules are adsorbed, they remain on the surface and do not desorb significantly. In general, the first-order kinetic constant increases with an increase in the initial concentration of the diesel oil. Higher concentrations of diesel oil mean more molecules of diesel oil are present, increasing the chances of collisions between diesel oil molecules and any other reactants.

3.6 Isotherm study

We performed an isotherm study on BPBC and the results are shown in Fig. 8. It was seen that the best-fit isotherm model is the BET isotherm. It has a high model R^2 value of 0.9898, demonstrating that the adsorbate molecules form a distinct layer on the

Table 2 Summary of kinetic data on banana peel biochar (BPBC) for diesel oil adsorption

Initial concentration (mg/L)	First-order kinetics			Second-order kinetics		
	k_1 (1/min)	q_e (g/g)	R^2	k_2 (L/mg-min)	q_e (g/g)	R^2
50	0.3135	4.7151	0.9700	0.0333	6.8820	0.9556
100	0.2614	6.5959	0.9599	0.0179	10.0246	0.9510
150	0.3584	6.2603	0.9544	0.0308	8.8868	0.9392
200	0.4043	6.1609	0.9634	0.0385	8.4793	0.9467
300	0.5185	5.9668	0.9827	0.0609	7.7440	0.9660
400	0.6569	5.8853	0.9844	0.0900	7.3213	0.9685
500	0.7971	5.8435	0.9797	0.1210	7.0756	0.9674

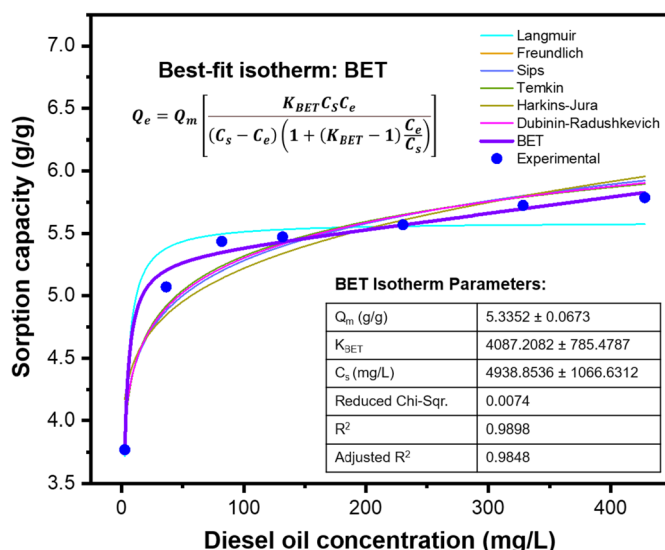


Fig. 8 Isotherm study on banana peel biochar (BPBC) for diesel oil adsorption

Table 3 Comparison of banana peel biochar (BPBC) diesel oil adsorption performance against other adsorbents

Adsorbent	Maximum sorption capacity (mg/g)	Isotherm model	Reference
Agar-carboxymethylcellulose-silver nanocomposite	12.26	Langmuir	(Ali et al. 2021)
Fe ₃ O ₄ /Bentonite/rGO	81.65	Sips	(Ewis et al. 2022)
Fe ₃ O ₄ /Bentonite/MWCNTs	77.12		
Crab-Shell-Derived Biochar	93.90	Freundlich	(Cai et al. 2019)
Crystalline calcite particles	333.30	Langmuir	(Wu et al. 2017)
Esterified durian peel adsorbent with stearic acid	378.00	Langmuir	(Nam et al. 2020)
Poly (methyl methacrylate) grafted wheat straw	1129.00	Freundlich	(Suresh et al. 2022)
Graphene oxide	1335.00	Freundlich	(Diraki et al. 2019)
Lignin-carbon foam	7842.71	Temkin	(Vannarath and Thalla 2021)
Banana peel biochar (BPBC)	5335.20	BET	This work

surface. Furthermore, it suggests that multilayer adsorption takes place in the system. Here, the Q_m is 5.3352 g/g, which is a relatively high sorption capacity compared to other adsorbents (Table 3). The BET isotherm has been proposed in several studies to fit their experimental data. According to the BET isotherm, an initial monolayer of adsorbate molecules will form on the adsorbent surface, and occasionally, further layers will grow on top of the monolayer. Multilayer adsorption is another possibility in which different layers of adsorbate molecules may stack on the monolayer. It is assumed that every adsorption site on the surface is heterogeneous, which implies that each one of them has a constant affinity for the adsorbate. However, the

site energies and surface properties of actual systems may differ from those predicted by the BET hypothesis (Ebadi et al. 2009). The BET isotherm makes the supposition that adsorbate molecules do not interact with one another on the surface and that their existence has no bearing on the adsorption procedure. The model also makes use of equilibrium conditions, homogenous adsorbent surfaces with comparable adsorption sites, ideal gas behavior, and weak intermolecular interactions between the molecules of the adsorbate and the adsorbent surface. This may indicate that the adsorption process has reached equilibrium, which would mean that the rates of adsorption and desorption are equal (Thommes et al. 2015).

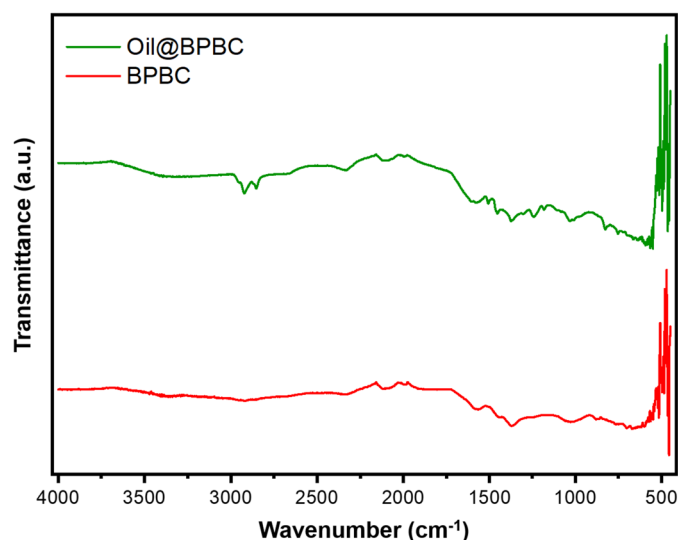


Fig. 9 Fourier transform infrared (FTIR) spectra of banana peel biochar (BPBC) before and after adsorption

3.7 Post-adsorption characterization

SEM images of BPBC after oil adsorption (Fig. 9) revealed that it has flake-like features with rough, irregular, uneven, and crater-like pores (Esther and Udochukwu 2022). The surface pores are open before adsorption and are already occupied after adsorption, as illustrated in Fig. S3 (Agha et al. 2019). Within the particles of the two biochars, there are pores of various diameters. The large pores are more easily accessible due to their size, indicating that the surface of the biochar was coated by oil following adsorption. However, SEM examination reveals that these macropores are the reason for the saturation (Khare et al. 2017).

The elemental composition of the results from before and after oil adsorption by energy-dispersive X-ray spectroscopy (EDX) is shown in Table S5. The elemental analysis of this biochar after adsorption shows 85.99% C, 0.34% Ca, 3.40% K, 7.47% O, 1.16% Cl, 0.02% P, 0.15% S and 1.46% N. Other elements, such as chlorine, phosphorus, and sulfur, remained constant before and after oil adsorption. The carbon content notably increased after diesel oil adsorption, which is expected because diesel oil is primarily made of hydrocarbons.

The BPBC before and after adsorption were tested using Fourier transform infrared spectroscopy (FTIR), and the results are shown in Fig. 9. The C=C stretching vibration of an α , β -unsaturated ketone from 1576 cm^{-1} in BPBC (before) to 1575 cm^{-1} in BPBC (after) carbon-carbon double bond next to a carbonyl group. An additional peak appeared at 1241 cm^{-1} after adsorption. This peak is associated with the C=O stretching of an aromatic compound and is due to aromatics in the adsorbed diesel oil.

Additional peaks at 1454 cm^{-1} are found in the BPBC after adsorption. These peaks are associated with C-H bending, which can be attributed to the adsorbed aromatics and substituted hydrocarbons in the BPBC after adsorption. Lastly, an additional peak at 2852 cm^{-1} and 2921 cm^{-1} was found after diesel oil adsorption. This peak indicates that the availability of functional groups for chemical reactions, adsorption, or surface modification can be characterized by C-H stretching vibrations associated with hydroxyl groups.

3.8 Comparison with other adsorbents

We compared the performance of the BPBC for removing diesel oil in water at optimum solution environmental conditions with other adsorbents used for diesel oil adsorption, and the results are tabulated in Table 3. BPBC derived from saba banana peels showed superior performance over other biochars, owing to the porosity and hydrophobicity of the BPBC. This suggests that BPBC can be used as an excellent adsorbent for diesel oil removal in water.

3.9 Adsorption mechanism

Here, we reported the use of saba banana peel biochar as an adsorbent for diesel oil removal in water. Through comprehensive characterization before and after adsorption, as well as isotherm and kinetic modeling, we deduce the adsorption mechanism happening during diesel oil adsorption.

Biochar is a carbon-rich material derived from the pyrolysis of biomass. Its porous structure and high surface area make it an effective adsorbent for various pollutants, including organic compounds like diesel oil. The

adsorption mechanism of biochar for diesel oil involves physical and chemical processes. Biochar has a network of pores that can physically trap diesel oil molecules. The larger mesopores and micropores in biochar provide sites where diesel oil molecules can be physically adsorbed. This is supported by our isotherm study, which fits well with the BET isotherm, suggesting multilayer adsorption. The high surface area and well-defined pore size distribution of biochar play a crucial role in adsorption. The accessibility of these pores allows for efficient adsorption of diesel oil molecules.

Biochar has a graphitic structure, as evidenced by XRD, with aromatic carbon rings, as seen from FTIR. Diesel oil contains aromatic hydrocarbons. The interaction between the aromatic rings in biochar and diesel oil molecules through π - π stacking and Van der Waals forces contributes to the adsorption. The hydrophobic nature of the biochar, as seen from contact angle measurements, promotes the adsorption process. Hydrophobic interactions occur between the nonpolar components of biochar and diesel oil, leading to the adsorption of the hydrophobic diesel oil molecules onto the biochar surface.

The biochar surfaces also contain functional groups with charges (e.g., oxygen-containing groups), as seen in FTIR. These charged sites can interact with polar components of diesel oil through electrostatic attraction, enhancing the adsorption capacity. Some functional groups on the biochar surface (such as oxygen-containing groups like hydroxyl and carboxyl groups) may undergo chemical reactions with certain components of diesel oil. This chemisorption involves covalent bonding or other chemical interactions, providing additional adsorption sites. This is supported by our kinetic study which is best fitted with the first-order model, suggesting chemisorption.

4 Conclusions

The comprehensive characterization of Banana Peel Biochar (BPBC) has provided valuable insights into its physical and chemical properties. SEM analysis revealed the porous structures of BPBC. EDX analysis confirmed the high potassium content in BPBC, consistent with previous studies on biochar derived from banana peel waste. FTIR identified the presence of specific functional groups on the surface of BPBC. DSC and TGA analyses showed the thermal stability of BPBC. BET experiments demonstrated that BPBC has a surface area comparable to other biochar but significantly greater micropore volume, indicating its potential as an efficient adsorbent. XRD analysis confirmed the presence of crystalline graphite in BPBC, indicative of graphitization during the pyrolysis process. Hydrophobicity

tests revealed the hydrophobic nature of BPBC due to its porous structure and the presence of specific functional groups. Based on the detailed characterization, BPBC shows promise as an effective adsorbent for various applications, particularly in oil-water separation. The investigation of adsorption parameters further elucidated the factors influencing the sorption capacity of BPBC for diesel oil removal from water. The study revealed that the sorption capacity of BPBC is influenced by the amount of adsorbent used, with an optimal dosage observed at 2.5g. The pH level of the solution minimally affects sorption capacity, with pH7 being the most favorable condition. The salinity of the aqueous solution positively affects the adsorption capacity of BPBC, with higher salinity levels corresponding to increased sorption capacity. Contact time between the adsorbent and diesel oil also plays a crucial role, with longer contact times leading to higher sorption capacities. Optimization of parameters identified the optimum conditions for diesel oil adsorption as 2.50g BPBC loading, pH7.00, 44,999.95 mg/L salinity, and 240 minutes of contact time. The first-order kinetics model provided a more accurate representation of the adsorption process, while the BET isotherm model was in good agreement with the experimental data, indicating multilayer adsorption on the BPBC surface. Characterization after adsorption revealed changes in surface properties and the presence of aromatic and oxygenated hydrocarbons in the adsorbed diesel oil. The diesel adsorption takes place primarily by pore-filling, π - π stacking, Van der Waals, electrostatic, and hydrophobic interactions, as well as chemisorption. These results contribute to the development of effective and sustainable strategies for oil spill cleanup and environmental remediation. Future research directions include more sophisticated characterization methods to fully understand the properties of BPBC. Moreover, understanding the mechanisms of adsorption through advanced analytical techniques and computer modeling can provide valuable insights into the chemical interactions between biochar and oil molecules.

Abbreviations

ANOVA	Analysis of variance
BET	Brunauer-Emmett-Teller
BC	Biochar
BPBC	Banana peel biochar
CCD	Central composite design
DSC	Differential scanning calorimetry
DTA	Differential thermal analysis
EDX	Energy dispersive X-ray spectroscopy
FTIR	Fourier transform infrared spectroscopy
SBPP	Saba banana peel powder
SEM	Scanning electron microscopy
TGA	Thermogravimetric analysis
XRD	X-ray diffraction

Supplementary Information

The online version contains supplementary material available at <https://doi.org/10.1007/s44246-024-00100-9>.

Additional file 1: Fig. S1. SEM images of saba banana peel powder (SBPP) at different magnifications. **Table S1.** Comparison of elemental analysis of saba banana peel powder (SBPP) and banana peel biochar (BPBC). **Table S2.** Summary of differential scanning calorimetry (DSC) results for saba banana peel powder (SBPP) and banana peel biochar (BPBC). **Table S3.** Summary of thermogravimetric differential thermal analysis (TG-DTA) results for saba banana peel powder (SBPP) and banana peel biochar (BPBC). **Table S4.** Analysis of variance for the reduced cubic model. **Fig. S2.** Kinetic study on banana peel biochar (BPBC) for diesel oil adsorption: (a) 50 mg/L, (b) 100 mg/L, (c) 150 mg/L, (d) 200 mg/L, (e) 300 mg/L, (f) 400 mg/L, and (g) 500 mg/L. **Table S5.** Comparison of elemental analysis of banana peel biochar (BPBC) before and after adsorption. **Fig. S3.** SEM images of banana peel biochar (BPBC) at different magnifications.

Authors' contributions

All authors contributed to the study's conception and design. Material preparation, data collection, and analysis were performed by Jefrick Jun Daniel T. Urgel, Justin Marwin A. Briones, Emmanuel Jr. B. Diaz, Kirstin Margaux N. Dimaculangan, Kayla L. Rangel, and Edgar Clyde R. Lopez. The first draft of the manuscript was written by Edgar Clyde R. Lopez and all authors commented on previous versions of the manuscript. All authors read and approved the final manuscript.

Funding

The authors did not receive support from any organization for the submitted work.

Availability of data and materials

The datasets used or analyzed during the current study are available from the corresponding author upon reasonable request.

Declarations

Competing interests

All authors certify that they have no affiliations with or involvement in any organization or entity with any financial interest or non-financial interest in the subject matter or materials discussed in this manuscript.

Author details

¹Chemical Engineering Department, Adamson University, San Marcelino St., Ermita, 1000 Manila, Philippines. ²Nanotechnology Research Laboratory, Department of Chemical Engineering, University of the Philippines Diliman, 1100 Quezon City, Philippines. ³Department of Chemical Engineering, University of Santo Tomas, España, 1015 Manila, Philippines.

Received: 5 October 2023 Revised: 7 January 2024 Accepted: 8 January 2024

Published online: 05 February 2024

References

- Agha SK, Priyatharshini S, Dhevagi P, Chitdeshwari T, Avudainayagam S (2019) Removal of Lead and cadmium from aqueous solutions by Banana Peel biochar. *Madras Agricult J* 106:1–3. <https://doi.org/10.29321/maj.2019.000220>
- Ali MA, Shaaban-Dessuuki SA, El-Wassefy NA, Mostafa SI, Hussein MH (2021) Adsorption of crude and waste diesel oil onto agar-carboxymethylcellulose-silver nanocomposite in aqueous media. *Inorg Chem Commun* 133:108915. <https://doi.org/10.1016/j.inoche.2021.108915>
- Ayeni AO, Daramola MO, Adetayo AE, Sekoai PT, Nwinyi OC, Ejekwu O (2020) Biological and non-biological methods for lignocellulosic biomass deconstruction. In *Green Energy Technol*. https://doi.org/10.1007/978-3-030-38032-8_7
- Bhardwaj N, Bhaskarwar AN (2018) A review on sorbent devices for oil-spill control. In *Environ Pollut* 243:1758–1771. <https://doi.org/10.1016/j.envpol.2018.09.141>
- Cai L, Zhang Y, Zhou Y, Zhang X, Ji L, Song W, Zhang H, Liu J (2019) Effective adsorption of diesel oil by crab-shell-derived biochar nanomaterials. *Materials* 12:2. <https://doi.org/10.3390/ma12020236>
- Dai Y, Zhang N, Xing C, Cui Q, Sun Q (2019) The adsorption, regeneration and engineering applications of biochar for removal organic pollutants: a review. *Chemosphere* 223:12–27. <https://doi.org/10.1016/j.chemosphere.2019.01.161>
- Diraki A, Mackey HR, Mckay G, Abdala A (2019) Removal of emulsified and dissolved diesel oil from high salinity wastewater by adsorption onto graphene oxide. *J Environ Chem Eng* 7:3. <https://doi.org/10.1016/j.jece.2019.103106>
- Ebadi A, Soltan Mohammadzadeh JS, Khudiev A (2009) What is the correct form of BET isotherm for modeling liquid phase adsorption? *Adsorption* 15:65–73. <https://doi.org/10.1007/s10450-009-9151-3>
- El-Nemr MA, Ismail IMA, Abdelmonem NM, El Nemr A, Ragab S (2021) Amination of biochar surface from watermelon peel for toxic chromium removal enhancement. *Chin J Chem Eng* 36:199–222. <https://doi.org/10.1016/j.cjche.2020.08.020>
- Elnour AY, Alghyama AA, Shaikh HM, Poulouse AM, Al-Zahrani SM, Anis A, Al-Wabel MI (2019) Effect of pyrolysis temperature on biochar micro-structural evolution, physicochemical characteristics, and its influence on biochar/polypropylene composites. *Appl Sci* 9(6):7–9. <https://doi.org/10.3390/app9061149>
- Ewis D, Mahmud N, Benamor A, Ba-Abbad MM, Nasser M, El-Naas M (2022) Enhanced removal of diesel oil using new magnetic bentonite-based adsorbents combined with different carbon sources. *Water Air Soil Pollut* 233:195. <https://doi.org/10.1007/s11270-022-05641-6>
- Goveas LC, Nayak S, Selvaraj R (2022) Concise review on bacterial degradation of petroleum hydrocarbons: emphasis on Indian marine environment. In *Bioresour Technol Rep* 19:101136. <https://doi.org/10.1016/j.biteb.2022.101136>
- Grisales-Cifuentes CM, Serna Galvis EA, Porras J, Flórez E, Torres-Palma RA, Ace- las N (2021) Kinetics, isotherms, effect of structure, and computational analysis during the removal of three representative pharmaceuticals from water by adsorption using a biochar obtained from oil palm fiber. *Bioresour Technol* 326:124753. <https://doi.org/10.1016/j.biortech.2021.124753>
- Haridharan N, Sundar D, Kurrupasamy L, Anandan S, Liu CH, Wu JJ (2022) Oil spills adsorption and cleanup by polymeric materials: a review. In *Polym Adv Technol* 33(5):1353–1384. <https://doi.org/10.1002/pat.5636>
- Khare P, Dilshad U, Rout PK, Yadav V, Jain S (2017) Plant refuses driven biochar: application as metal adsorbent from acidic solutions. *Arab J Chem* 10:53054–53063. <https://doi.org/10.1016/j.arabjch.2013.11.047>
- Kumar A, Bhattacharya T (2021) Biochar: a sustainable solution. In *Environ Develop Sustain* 23(5):6642–6680. <https://doi.org/10.1007/s10668-020-00970-0>
- Kumar V, Kumar M, Prasad R (2019) Microbial action on hydrocarbons. In *Microb Act Hydrocarbons*. <https://doi.org/10.1007/978-981-13-1840-5>
- Nam T, Van Nguyen TT, Dung DN, Phuong PTH (2020) Esterified durian peel adsorbents with stearic acid for spill removal. *Chem Eng Trans* 78:271–276. <https://doi.org/10.3303/CET2078046>
- Omulo G, Banadda N, Kabenge I, Seay J (2019) Optimizing slow pyrolysis of banana peels wastes using response surface methodology. *Environ Eng Res* 24(2):354–361. <https://doi.org/10.4491/EER.2018.269>
- Pallewatta S, Samarasekera SM, Rajapaksha AU, Vithanage M (2023) Oil spill remediation by biochar derived from bio-energy industries with a pilot-scale approach during the X-press pearl maritime disaster. *Mar Pollut Bull* 189:114813. <https://doi.org/10.1016/j.marpolbul.2023.114813>
- Patel S, Homaei A, Patil S, Daverey A (2019) Microbial biosurfactants for oil spill remediation: pitfalls and potentials. In *Appl Microbiol Biotechnol* 103:27–37. <https://doi.org/10.1007/s00253-018-9434-2>
- Qiao K, Tian W, Bai J, Wang L, Zhao J, Du Z, Gong X (2019) Application of magnetic adsorbents based on iron oxide nanoparticles for oil spill remediation: a review. *J Taiwan Inst Chem Eng* 97:227–236. <https://doi.org/10.1016/j.jtice.2019.01.029>

- Selvarajoo A, Oochit D (2020) Effect of pyrolysis temperature on product yields of palm fibre and its biochar characteristics. *Mater Sci Energy Technol* 3:575–583. <https://doi.org/10.1016/j.mset.2020.06.003>
- Sial TA, Khan MN, Lan Z, Kumbhar F, Ying Z, Zhang J, Sun D, Li X (2019) Contrasting effects of banana peels waste and its biochar on greenhouse gas emissions and soil biochemical properties. *Process Saf Environ Prot* 122:366–377. <https://doi.org/10.1016/j.psep.2018.10.030>
- Silva WO, Nagar B, Soutrenon M, Girault HH (2022) Banana split: biomass splitting with flash light irradiation. *Chem Sci* 13(6):1774–1779. <https://doi.org/10.1039/d1sc06322g>
- Silvani L, Vrchotova B, Kastanek P, Demnerova K, Pettiti I, Papini MP (2017) Characterizing biochar as alternative sorbent for oil spill remediation. *Sci Rep* 7:43912. <https://doi.org/10.1038/srep43912>
- Sinanoglou VJ, Tsiaka T, Aouant K, Mouka E, Ladika G, Kritsi E, Konteles SJ, Ioannou AG, Zoumpoulakis P, Strati IF, Cavouras D (2023) Quality assessment of Banana ripening stages by combining analytical methods and image analysis. *Appl Sci* 13(6):3533. <https://doi.org/10.3390/app13063533>
- Sun K, Ro K, Guo M, Novak J, Mashayekhi H, Xing B (2011) Sorption of bisphenol a, 17 α -ethinyl estradiol and phenanthrene on thermally and hydrothermally produced biochars. *Bioresour Technol* 102(10):5757–5763. <https://doi.org/10.1016/j.biortech.2011.03.038>
- Suresh K, Islam MA, Rastga M, Mohammadnezhad A, Fleck BA, Sadrzadeh M (2022) Poly (methyl methacrylate) grafted wheat straw for economical and eco-friendly treatment of oily wastewater. *Cellulose* 29(6):3351–3374. <https://doi.org/10.1007/s10570-022-04481-1>
- Thommes M, Kaneko K, Neimark AV, Olivier JP, Rodriguez-Reinoso F, Rouquerol J, Sing KSW (2015) Physisorption of gases, with special reference to the evaluation of surface area and pore size distribution (IUPAC technical report). *Pure Appl Chem* 87(9–10):1051–1069. <https://doi.org/10.1515/pac-2014-1117>
- Vannarath A, Thalla AK (2021) Synthesis and characterisation of an ultra-light, hydrophobic and flame-retardant robust lignin-carbon foam for oil-water separation. *J Clean Prod* 325:129263. <https://doi.org/10.1016/j.jclepro.2021.129263>
- Wei Z, Wei Y, Liu Y, Niu S, Xu Y, Park JH, Wang JJ (2024) Biochar-based materials as remediation strategy in petroleum hydrocarbon-contaminated soil and water: performances, mechanisms, and environmental impact. In *J Environ Sci* 138:350–372. <https://doi.org/10.1016/j.jes.2023.04.008>
- Wu MN, Maity JP, Bundschuh J, Li CF, Lee C, Hsu CM, Lee WC, Huang CH, Chen CY (2017) Green technological approach to synthesis hydrophobic stable crystalline calcite particles with one-pot synthesis for oil–water separation during oil spill cleanup. *Water Res* 123:332–344. <https://doi.org/10.1016/j.watres.2017.06.040>
- Zhao J, Li Q, Wang Q, Zhang J, Sun X, Zhang W, Lu C (2023) Facile construction of robust and powerful biochar-decorated porous foams with superwettability for automatic and continuous oil spill remediation. *Ind Eng Chem Res* 62(17):6697–6706. <https://doi.org/10.1021/acs.iecr.3c00173>

Publisher's Note

Springer Nature remains neutral with regard to jurisdictional claims in published maps and institutional affiliations.